

## Spin-dependent electron-hole capture kinetics in conjugated polymers

Stoyan Karabunarliev and Eric R. Bittner<sup>†</sup>

Department of Chemistry, University of Houston, Houston, TX 77204-5003

(Dated: March 22, 2024)

The recombination of electron-hole pairs injected in extended conjugated systems is modeled as a multipathway vibron-driven relaxation in monoexcited state-space. The computed triplet-to-singlet ratio of exciton formation times  $r = \tau_T = \tau_S$  increases from 0.9 for a model dimer to 2.5 for a 32-unit chain, in excellent agreement with experiments. Therewith we rationalize recombination efficiency in terms of spin-dependent interstate vibronic coupling and spin- and conjugation-length-dependent exciton binding energies.

PACS numbers: 78.60.Fi, 73.61.Ph, 82.20.Wt

**Introduction** – The efficiency of electroluminescence (EL) from conjugated polymers in light emitting diodes (LEDs) is largely determined by the fraction of injected electron-hole (e-h) pairs which combine to form emissive spin-singlet (S) as opposed to non-emissive spin-triplet (T) bound states.[1] If one assumes that the cross sections for S and T e-h captures are equivalent  $\sigma_S = \sigma_T$ , then the singlet generation fraction  $\phi_S = \sigma_S / (\sigma_S + 3\sigma_T)$  will be limited to 25% according to spin multiplicity. Nonetheless, efficiencies corresponding to  $\phi_S$  over 50% have been achieved in poly(p-phenylenevinylene) (PPV) based LEDs.[2, 3] From this it has been inferred that singlet e-h capture is intrinsically more efficient than the respective triplet process,  $\sigma_S > \sigma_T$ . Recent PA/PADMR experiments on a wide variety of conjugated systems indicate that the cross-section ratio  $r = \sigma_S / \sigma_T$  typically lies between 2 and 5, [4] and that the ratio increases with conjugation length.[5]

The observed variation of  $r$  was originally related [5] to the optical gap according to an interchain recombination model[6]; however, more recent experiments indicate that large values of  $r$  are characteristic of extended intrachain conjugation.[5, 7] Wilson et al. have measured  $\sigma_S$  and  $\sigma_T$  consistent with  $r \approx 4$  for a polymer, but only  $r \approx 0.9$  for the monomer.[7] While time-dependent scattering calculations by Kobrak and Bittner[8] indicate that the weakly bound  $S_1$  exciton is a more efficient trap of free e-h pairs than the tightly bound  $T_1$  triplet exciton, the systematic variation of  $r$  with (effective) conjugation length  $n$  has remained unclear.

This Letter addresses the kinetics of e-h capture in extended conjugated systems. To our best knowledge, ours is the first molecular-based approach which consistently reproduces the spin- and conjugation-length dependence of the process, and rationalizes it in terms of exciton binding energies. This has important ramifications in the design and synthesis of polymer materials for device applications.

**Method** – We simulate the recombination process in nondegenerate  $n$ -chains by the dissipative dynamics of the multi-level electronic system coupled to the phonon bath. The detailed structure of the Hamiltonian with a

general form

$$\hat{H} = \hat{H}_{el} + \hat{H}_{ph} + \hat{H}_{el-ph}; \quad (1)$$

is described in a separate publication,[9] and we mention only those salient features that are relevant herein. The electronic part  $\hat{H}_{el}$  reflects the configuration interaction (CI) of single excitations for a generic two-band polymer in a localized basis.[10, 11] The configurations  $j\mathbf{n}i = \sum_m \bar{c}_m^\dagger c_m |j\rangle$  taken over valence and conduction-band Wannier functions  $\bar{c}_m^\dagger$  and  $c_m$  represent geminate ( $\bar{m} = m$ ) and charge-transfer ( $\bar{m} \neq m$ ) e-h pairs.  $\hat{H}_{el}$  is parameterized from the  $n$ -band structure of extended PPV. Since the conjugated backbone is alternating, one-body CI integrals  $F_{m\mathbf{n}} = \sum_{\bar{m}} \bar{c}_m^\dagger F_{m\mathbf{n}} c_{\bar{m}} = \sum_{\bar{m}} \bar{c}_m^\dagger F_{\bar{m}\mathbf{n}} c_{\bar{m}}$  of the band structure operator  $\hat{F}$  obey electron-hole symmetry with  $\bar{F}_r = F_r$ . Spin dependency originates from two-body interactions with  $V_{m\mathbf{n}} = \sum_{\bar{m}} \bar{c}_m^\dagger V_{m\mathbf{n}} c_{\bar{m}} + 2 \sum_{\bar{m}} \bar{c}_m^\dagger V_{m\mathbf{n}} c_{\bar{m}}$  for singlets and  $V_{m\mathbf{n}} = \sum_{\bar{m}} \bar{c}_m^\dagger V_{m\mathbf{n}} c_{\bar{m}}$  for triplets. Assuming zero-differential overlap except for geminate orbitals, we take into account only true Coulomb and exchange terms  $\sum_{\bar{m}} \bar{c}_m^\dagger V_{m\mathbf{n}} c_{\bar{m}}$  and  $\sum_{\bar{m}} \bar{c}_m^\dagger V_{m\mathbf{n}} c_{\bar{m}}$ , and (transition) dipole-dipole interactions  $\sum_{\bar{m}} \bar{c}_m^\dagger V_{m\mathbf{n}} c_{\bar{m}}$  between geminate singlet pairs. The electron-phonon coupling term  $\hat{H}_{el-ph}$  assumes that localized conduction/valence levels  $f_0$  and nearest-neighbor transfer integrals  $f_1$  are modulated by lattice oscillations. Correspondingly, the phonon term consists of two sets of interacting local oscillators, giving rise to two dispersed optical phonon branches centered at 1600 and 100  $\text{cm}^{-1}$ , respectively. These frequencies roughly correspond to the C=C bond stretches and ring torsions in PPV, which largely dominate the Franck-Condon activity of the lowest optical transitions.[12, 13] Thus, by empirical adjustment of el-ph coupling strength in  $\hat{H}_{el-ph}$ , we compute in Condon approximation [13] fairly accurate absorption and emission band-shapes for PPV chains, reflecting conjugation-length dependence, vibronic structure and Stokes shifts.

Diagonalizing  $\hat{H}_{el}$  and  $\hat{H}_{ph}$  yields vertical excited states with energies  $\epsilon_a^0$  [14] and normal modes with frequencies  $\omega_l$ , which allow us to transform the el-ph cou-

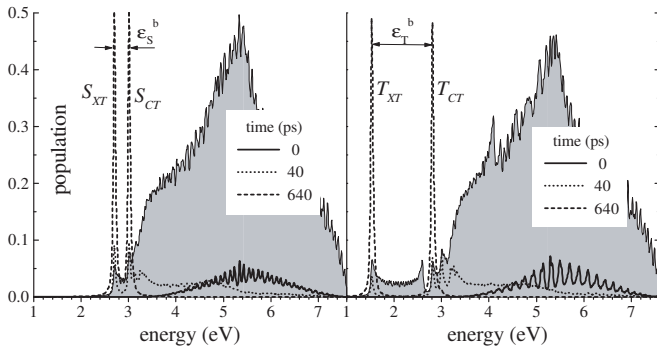


FIG. 1: Density of spin-singlet (left) and spin-triplet (right) states for PPV<sub>32</sub> (shaded area) and their populations at different recombination stages. The  $t = 0$  population corresponds to the initially injected e-h pair.

pling term in its diabatic representation.

$$\hat{H} = \sum_a \langle a | \hat{H} | a \rangle + \frac{1}{2} \sum_a \langle a | \hat{Q}^2 + \hat{P}^2 | a \rangle + \sum_{ab} g_{ab}^o \hat{Q} | a \rangle \langle b | \quad (2)$$

FIG. 1 shows the S and T densities of states (DOS) for a conjugated chain with  $n = 32$  repeat units (PPV<sub>32</sub>), obtained as a convolution of Lorentzian line-shapes with  $\Gamma = 0.01\text{eV}$ . We note that in singlet state-space, optical coupling with the ground state is concentrated mainly around the DOS bottom since only  $S_1$  and other low-lying excitonic states contain geminate configurations with transition dipoles in additive combinations.[9] Nonequilibrium dynamics in excited state-space is derived further from the diabatic interstate vibronic couplings  $g_{ab}$ . Assuming that phonons thermalize rapidly on the time scale of electronic relaxation, internal conversion (IC) rates  $k_{ab}$  for one-phonon processes are obtained in Markov approximation.[15]

$$k_{ab} = \sum_i \frac{(g_{ab}^o)^2}{\Gamma} (n_i + 1) \langle i | \hat{Q} | a \rangle \langle b | \quad (3)$$

Here  $n_i$  is the Bose-Einstein distribution of phonons at  $T = 300\text{K}$  and  $\Gamma$  is the empirical broadening. Note that for an elementary  $a \rightarrow b$  conversion to occur there must a phonon mode  $i$  close to the transition frequency  $\omega_{ab} = (\omega_a^o - \omega_b^o)/\hbar$ . Singlet and triplet superposition states are separately evolved in time according to the quantum master equation for the density matrix in energy representation,

$$\dot{\rho}_{ab} = -i \langle a | \hat{H} | b \rangle \rho_{ab} + \sum_{cd} R_{ab;cd} \rho_{cd} \quad (4)$$

where we decouple populations  $\rho_{aa}$  from coherences  $\rho_{ab}$  according to the Bloch model.[15]

$$\dot{R}_{aa;bb} = -k_{ab} \rho_{ab} + \sum_c k_{ac} \rho_{ac} \quad (5)$$

$$R_{ab;ab} = \frac{1}{2} \sum_c (k_{ac} + k_{bc}) \quad (6)$$

Results—Equations (3-6) allow us to model the relaxation of an arbitrary monoexcitation, including that with an electron and hole injected into the far ends of the conjugated chain. The resulting initial population of the DOS is shown in FIG. 1. We show as well the populations at an early relaxation time (40ps), and at 640ps when a stationary state is reached. In both spin-spaces, half of the population density propagates down to the lowest excitons ( $S_{XT}$  or  $T_{XT}$ ),[16] but the other half remains locked in metastable charge-transfer (CT) states ( $S_{CT}$  or  $T_{CT}$ ). The branching of the relaxation pathways is due to e-h symmetry, which separates excited states into even and odd under e-h transposition. The XT states, which are the lowest even ones, are not vibronically coupled with the CT states, which the lowest odd ones. XT and CT states are ultimately populated equally because the initial separated e-h pair is a 1:1 mixture of eigenstates with even and odd e-h parity. The weak e-h symmetry breaking of real conjugated systems is further modeled by slight conduction/valence band nonsymmetry according to the relation  $f_c = f_v = 1:1$ . The perturbation barely affects the DOS, but invokes weak vibronic coupling between the states of odd and even types, so that they undergo slow mutual conversions. The time-dependent XT and CT populations are shown in FIG. 2 both for the symmetric (a) and nonsymmetric (b) cases. We see that when e-h symmetry is broken, the fast formation of XT and CT during the first 100-200ps is followed up by a slow CT  $\rightarrow$  XT relaxation. Most notably, in comparison with the symmetric case, the initial XT-CT branching ratio changes drastically in favor of  $S_{XT}$  for singlets and in disfavor of  $T_{XT}$  for triplets. The subsequent  $S_{CT} \rightarrow S_{XT}$  relaxation is also substantially faster than the respective  $T_{CT} \rightarrow T_{XT}$  conversion process, and  $S_{XT}$  population remains about twice as high as that of  $T_{XT}$  throughout the simulated time-range. We note here that CT states are barely spin-dependent (see FIG. 1) due to negligible spin-exchange; hence S  $\rightarrow$  T intersystem crossing pre-equilibrium of long-lived CT states is also likely to occur prior to nule-h binding. As shown in FIG. 2a,  $S_{XT}$  formation proceeds notably faster than that of  $T_{XT}$ . Since even under e-h symmetry population buildup deviates from first-order kinetics in early stages when intermediate states are formed (see FIG. 1), we measure the relative efficiency of exciton formation by the time at which XT population reaches 40%. Thus for PPV<sub>32</sub> we find  $t_s = 109\text{ps}$  and  $t_t = 263\text{ps}$ , which corresponds to  $r = t_t/t_s = 2.5$  or  $\eta_s = 45\%$  in good agreement with both EL [2, 3] and PA/PADMR [4, 5] data. Singlet versus triplet recombination enhancement is related to the difference in exciton binding energies,[17] which we measure by  $\eta^b = \omega_{CT}^o / \omega_{XT}^o$ . Whereas  $S_{XT}$  is slightly lower than  $S_{CT}$ , spin-exchange contributes 1eV more to the

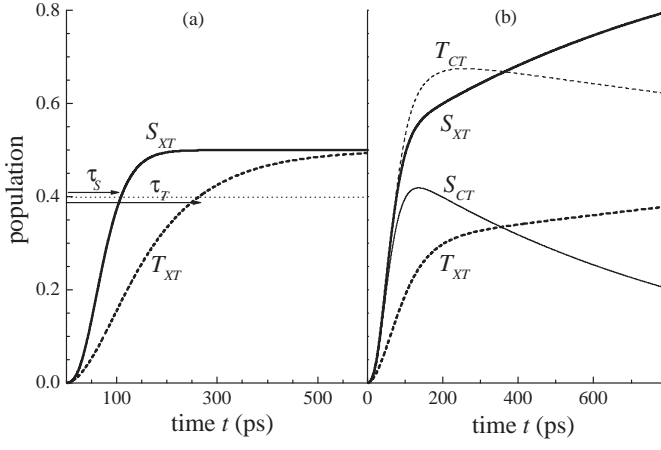


FIG. 2: Essential-state populations as a function of time for PPV<sub>32</sub> with strict (a) and weakly broken (b) e-h symmetry. The  $S_{CT}$  and  $T_{CT}$  populations not shown in (a) follow closely the  $S_{XT}$  curve.

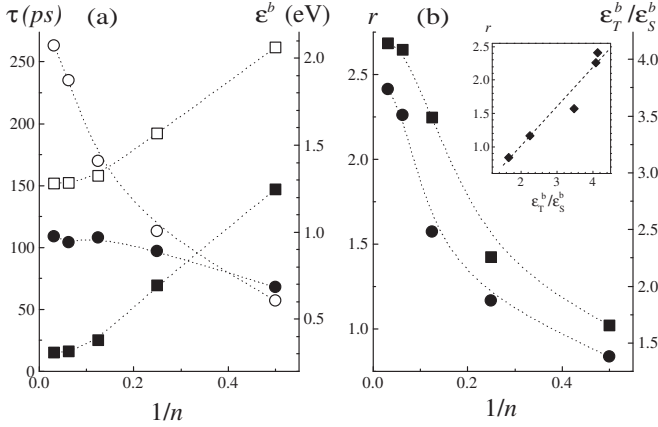


FIG. 3: (a) Variation of singlet and triplet binding energies and formation times with inverse conjugation length  $1/n$ . ( $\tau_S = \tau$ ,  $\tau_T = \tau$ ,  $\epsilon_S^b = \epsilon$ ,  $\epsilon_T^b = \epsilon$ ). (b) Binding energy and formation-time ratio  $r = \tau_T/\tau_S$  and binding-energy ratio  $\epsilon_T^b/\epsilon_S^b$  vs.  $1/n$ . Inset:  $r$  vs.  $\epsilon_T^b/\epsilon_S^b$ . Dashed curves are guides for the eye.

triplet binding energy  $\epsilon_T^b$ . Therefore relaxation into  $T_{XT}$  takes on the average a longer sequence of internal conversions, whose energy cutoff at 0.2 eV is determined by the phonon spectrum. If we assume that relaxation time is proportional to the dissipated energy and reciprocal to the mutual coupling of the states along the pathway, we can write down,

$$r = \frac{\tau_T}{\tau_S} / r_{vib} \frac{\epsilon_T^b}{\epsilon_S^b} \quad (7)$$

where  $r_{vib}$  reflects any difference of the effective vibronic coupling in S and T state-space. We further probe relation (7) by varying the conjugation length  $n$ . For the sake of brevity, results for the series of PPV model chains

with  $n = 2, 4, 8, 16$ , and 32 are summarized in FIG. 3a, where exciton binding energies  $\epsilon^b$  and formation times are plotted vs. inverse chain length  $1/n$  as commonly adopted. Note that  $\epsilon_S^b$  and  $\epsilon_T^b$  decrease in parallel with  $1/n$  and converge yet for the longest chains, suggesting that effective conjugation length is over 10 repeat units. Exciton formation times show different behavior. Whereas  $\tau_T$  increases about four times on going from the dimer to PPV<sub>32</sub>,  $\tau_S$  increases only slightly. In FIG. 3b we plot  $r$  vs.  $1/n$  and establish an excellent agreement with experiments [5, 7] for both oligomers and polymers, including a notable triplet enhancement with  $r = 0.9$  for  $n = 2$ . The inset is a plot of  $r$  vs.  $\epsilon_T^b/\epsilon_S^b$ , which illustrates the existence of a rough linear relationship (7) with  $r_{vib}$  similar to 0.6.

**Conclusion** – In summary, we have proposed and modeled an intrachain e-h recombination mechanism for conjugated systems, with computational results consistent with the spin-resolved experiments in all essential points. The model reflects the notion that exciton formation occurs via vibron-mediated internal conversions across excited states, and hence the overall rate of electronic relaxation is inversely proportional to the energy dissipated into vibrons. Hence while strong vibronic coupling of the lowest triplet is responsible for  $r < 1$  in short chains and molecular species, the disproportion of exciton binding energies accounts for the large  $r$  values in extended polymers. The approximate e-h symmetry of conjugated systems implies the parallel formation of long-lived charge-transfer states, which are nearly spin-independent, and thus susceptible to intersystem crossing prior to final spin-singlet enhanced e-h binding.

This work was funded by the National Science Foundation (CAREER Award) and the Robert A. Welch Foundation.

- 
- em ail: karabunarliev@uh.edu  
y em ail: bittner@uh.edu
- [1] R. H. Friend et al, Nature 397, 121 (1999).
  - [2] Y. Cao et al, Nature 397, 414 (1999).
  - [3] J. S. Kim et al, J. Appl. Phys. 88, 1073 (2000).
  - [4] M. Wohlgenannt et al, Nature 409, 494 (2001).
  - [5] M. Wohlgenannt et al, Phys. Rev. Lett. 88, 197401 (2002)
  - [6] Z. Shuai et al, Phys. Rev. Lett. 84, 131 (2000); A. Ye et al, Phys. Rev. B 65, 5208 (2002).
  - [7] J. S. Wilson et al, Nature 413, 828 (2001).
  - [8] M. Kobrak and E. R. Bittner, Phys. Rev. B 62, 11473 (2000).
  - [9] S. Karabunarliev and E. R. Bittner, cond-mat/0206015.
  - [10] D. Mukhopadhyay et al, Phys. Rev. B 51, 9476 (1995); M. Chandross et al, Phys. Rev. B 59, 4822 (1999).
  - [11] P. Karadakov et al, J. Chem. Phys. 94, 8520 (1991).
  - [12] T. W. Hagler et al, Phys. Rev. B 49, 10968 (1994); K. Pichler et al, J. Phys. Cond. Mat. 5, 7155 (1993); J.

- Comile et al, Chem .Phys.Lett. 278, 139 (1997).
- [13] S. Karabunarliev et al, J. Chem . Phys. 113, 11372 (2000); 114, 5863 (2001).
- [14] Superscript  $^{\circ}$  applies to quantities, taken at ground-state equilibrium .
- [15] For a recent review see: V .M ay and O .K uhn, Charge and Energy Transfer Dynamics in Molecular Systems (W iley-VCH , Berlin, 2000).
- [16] By  $S_{X\ T}$  we mean  $S_1$  and the several other thermally populated singlet states above it. Similarly for  $S_{C\ T}$ ,  $T_{X\ T}$ , and  $T_{C\ T}$ .
- [17] J. L .B redas, J. C omill, and A . J. H eeger, Adv. M ater. 8, 447 (1996); J. L .B redas et al, Acc. Chem . Res. 32, 267 (1999).